Journal of Crystal Growth 377 (2013) 1–8

Contents lists available at SciVerse ScienceDirect

Journal of Crystal Growth

journal homepage: www.elsevier.com/locate/jcrysgro

Measurements of surface attachment kinetics for faceted ice crystal growth

Kenneth G. Libbrecht *, Mark E. Rickerby

Department of Physics, California Institute of Technology, 264-33 Caltech, Pasadena, CA 91125, United States

ARTICLE INFO

Article history:
Received 18 February 2013
Received in revised form
8 April 2013
Accepted 20 April 2013
Communicated by T. Nishinaga
Available online 29 April 2013

Keywords:
A1. Growth models
A1. Crystal morphology
A1. Nucleation
A1. Surface structure
A2. Growth from vapor
A2. Single crystal growth

ABSTRACT

We present new measurements of the growth rates of faceted ice crystals in the temperature range $-40 < T < -2$ °C, from which we infer the surface attachment coefficients for the two principal facets. Our data are well described by a polynucleation model, allowing a determination of the molecular step energy as a function of temperature for both facets. These results are a substantial improvement over previous work, and we present an analysis showing that the inconsistencies seen in prior measurements could be explained by systematic errors associated with diffusion effects and substrate interactions. These data provide new insights into the surface attachment kinetics governing ice crystal growth, and they suggest new avenues for examining ice growth behavior using molecular dynamics simulations. Knowledge gained by a detailed case study of ice may in turn lead to a greater general understanding of the fundamental physics underlying crystal growth dynamics.

1. Introduction

Crystal growth is typically governed by a broad range of physical processes over many length scales. These include transport phenomena in the material surrounding the crystal, such as heat and particle diffusion, as well as the detailed attachment kinetics that control how molecules become part of the crystalline lattice. The attachment kinetics are especially difficult to model, since the many-body molecular dynamics at the surface can include numerous subtle and nontrivial effects. Advances in materials science are often hindered by uncertainties in crystal growth behavior, so developing a fuller understanding of surface attachment kinetics remains an important goal.

We have been exploring ice crystal growth as a case study for investigating surface attachment kinetics. Ice plays significant roles in many environmental and biological processes, plus the intermolecular potentials between water molecules have been well studied, allowing sophisticated *ab initio* molecular dynamics simulations of the ice surface structure and growth [1–4]. Ice is also well suited for investigating chemical effects on crystal growth dynamics, since there is a substantial literature on ice surface chemistry, including solvation effects that may be relevant to crystal growth catalysis [5,6].

Ice crystal growth from water vapor exhibits a rich phenomenology that remains rather poorly understood [7]. For example, the morphology of growing ice crystals changes dramatically with temperature, showing several transitions between plate-like and columnar structures. These observations suggest a complex temperature dependence in the attachment kinetics, as well as indicating substantial differences in surface structure and/or dynamics on the principal facets.

A key experimental goal for understanding the attachment kinetics in ice is to establish accurate measurements of crystal growth behaviors under well-defined conditions. Of particular interest are the growth rates $v(T, \sigma_{surf})$ of the two principal facets, for each giving the perpendicular surface growth velocity as a function of temperature and supersaturation at the surface. It is often convenient to write $v(T, \sigma_{surf}) = \alpha(T, \sigma_{surf}) v_{kin}(T) \sigma_{surf}$, where $v_{kin}(T)$ is a temperature-dependent "kinetic" velocity derived from statistical mechanics [7]. The dimensionless attachment coefficient α then encapsulates the molecular kinetics governing crystal growth at the solid/vapor interface. From the definition of v_{kin}, we must have $\alpha \leq 1$.

Comparing measurements of α with crystal growth theory immediately yields basic information about the ice surface structure and the underlying molecular processes defining the attachment kinetics. For example, observing a functional form $\alpha(\sigma_{surf}) \sim \exp(-\sigma_0/\sigma_{surf})$, where σ_0 is a constant, is strong evidence that the growth is limited mainly by the nucleation of molecular layers [8]. Alternatively, finding $\alpha(\sigma_{surf}) \sim \sigma_{surf}$ (or equivalently,

* Corresponding author. Tel.: +1 626 395 3722.
E-mail address: kgl@caltech.edu (K.G. Libbrecht).

0022-0248/$ - see front matter © 2013 Elsevier B.V. All rights reserved.
http://dx.doi.org/10.1016/j.jcrysgro.2013.04.037

$v(\sigma_{surf}) \sim \sigma_{surf}^2$) suggests that screw dislocations are the dominant source of molecular steps, while observing $\alpha \approx 1$ suggests a rough surface with fast attachment kinetics [8].

Evidence that layer nucleation is the dominant factor in ice attachment kinetics has been building for many years, suggesting that dislocations play at most a minor role in determining basic ice growth behaviors (see the discussion in [9]). A polynucleation (birth-and-spread) model is then expected to describe the growth of large surfaces with high nucleation rates, as is typical in many ice growth experiments. This picture has been further supported by direct observations of the nucleation and growth of individual islands on the ice basal and prism facets [10]. For the polynucleation model we write the parameterization $\alpha(\sigma_{surf}) = A \exp(-\sigma_0/\sigma_{surf})$, where A is at most a weakly varying function of σ_{surf} [8].

Experiments measuring $\alpha(T, \sigma_{surf})$, or related quantities, have been reported in numerous investigations over many decades. Morphological studies, for example, have observed ice growth from water vapor in air as a function of T and σ_∞, where σ_∞ is the supersaturation far from the growing crystals. Beginning with the pioneering work of Nakaya [11], different morphological studies have been in reasonably good agreement, the results being refined and extended over time (see [12] and references therein).

These morphological observations alone, however, are not satisfactory for quantitative studies of the physics underlying ice attachment kinetics. The observations are typically done in air at atmospheric pressure, so $\sigma_{surf} \ll \sigma_\infty$ from diffusion effects, and reliably estimating σ_{surf} under such conditions can be exceedingly difficult, as we discuss below. Although much useful information about growth anisotropies and atmospheric phenomenon can be gleaned from morphological studies, quantitative estimates of $\alpha(T, \sigma_{surf})$ from these experiments are highly uncertain.

Experiments measuring $\alpha(T, \sigma_{surf})$ more directly have not enjoyed the same reasonable consensus as the morphological studies, however, as we examine below. Quantitative measurements of $v(T, \sigma_{surf})$ have varied considerably between different experiments, and even the functional form of $v(\sigma_{surf})$ at different temperatures and on different facets has not been on a firm observational footing. A long-sought goal has been to use precise measurements of $\alpha(T, \sigma_{surf})$ to discover the physical mechanisms underlying the temperature transitions seen in ice growth morphologies [13,14,7]. To date, however, this goal has not been realized, in part because the measurements have not been sufficiently accurate.

In the following section we discuss a series of known systematic errors that can affect ice growth measurements, and examine their effects on previous experiments. We conclude that these systematic errors are substantially more important than was previously realized, and that essentially all of the past experiments have been affected to some degree. Our analysis suggests that these often-underappreciated systematic errors are able to explain the substantial discord between the different measurements of $v(T, \sigma_{surf})$.

Following this, we then report the development of a new ice growth experiment that eliminates or greatly reduces these known systematic effects. Measurements of α are reported for both the prism and basal facets over a range of conditions. With careful management of the experimental systematics, our data show excellent internal consistency and reproducibility, and we believe that our measurements of $\alpha(T, \sigma_{surf})$ are a marked improvement over previous attempts. We conclude with a discussion of the theoretical consequences of these new results regarding the ice surface structure and growth dynamics.

2. Measuring kinetic coefficients

The usual experimental method for determining $\alpha(T, \sigma_{surf})$ is to measure growth velocities under known conditions and then use $\alpha(T, \sigma_{surf}) = v(T, \sigma_{surf})/v_{kin}\sigma_{surf}$. We begin our discussion with a quantitative examination of several known sources of systematic errors in such measurements, and we examine their possible effects on previous experiments.

2.1. Diffusion effects

Ice growth measurements have often been done in air, and in this circumstance it is well known that the growth rates are partially limited by water vapor diffusion through the air. The experimenter typically only controls and/or measures σ_∞, the supersaturation far from the growing crystal, so σ_{surf} must be inferred indirectly. To quantify the relation between σ_{surf} and σ_∞, it is useful to examine the growth of a spherical ice crystal, since in that case one has a relatively simple analytic solution to the diffusion equation [15,7]. In air this gives

$$\sigma_{surf} = \frac{\alpha_{diff}}{\alpha + \alpha_{diff}} \sigma_\infty \tag{1}$$

for the isothermal case, where $\alpha_{diff} \approx 0.15/pR_{\mu m}$, $R_{\mu m}$ is the sphere radius in microns, $p = P/P_{atm}$, P is the background air pressure, and $P_{atm} = 1$ bar [7].

In the limit $\alpha \ll \alpha_{diff}$ we have $\sigma_{surf} \approx \sigma_\infty$, so the growth is primarily limited by attachment kinetics. In the opposite limit, $\alpha_{diff} \ll \alpha$, the growth is mainly limited by particle diffusion, giving $v \approx v_{diff} = \alpha_{diff} v_{kin} \sigma_\infty$, which is independent of α. When the growth is mainly diffusion-limited, it can be exceedingly difficult to use growth measurements to extract useful information about α, since even small uncertainties in measurements of σ_∞ or v result in large errors in the inferred σ_{surf} and α.

Even if $p \ll 1$, we have found that diffusion effects can affect the interpretation of ice growth measurements. For example, if a slowly growing test crystal has a fast-growing neighbor crystal, then the neighbor may substantially perturb the supersaturation field near the test crystal, and determining the size of the perturbation is nontrivial. The best way to avoid this problem is to observe only well isolated test crystals, with no neighboring crystals between the test crystal and the outer boundary where σ_∞ is determined.

Even with well isolated test crystals, fast growing neighboring facets can significantly affect the behavior of slower growing facets, again via a perturbation of the supersaturation field around the crystal. For small perturbations when $p \ll 1$, we have used an approximate correction to σ_{surf}

$$\sigma_{surf} \approx \sigma_\infty - \sum_i \frac{f_i v_i}{\alpha_{diff} v_{kin}} \tag{2}$$

where f_i is the area of a growing region of the crystal, v_i is the growth velocity of that region, α_{diff} is calculated using an approximate effective radius for the crystal, and the sum is over the entire exposed area of the crystal. It is straightforward to show that Eq. (2) gives a reasonable approximate correction provided $\Delta\sigma/\sigma_\infty \ll 1$, where $\Delta\sigma$ equals the sum in the expression. Eq. (2) is especially useful for estimating residual diffusion corrections in low-pressure growth data, since $\Delta\sigma$ is readily computed from experimentally derived quantities.

Morphological studies have typically been done with $p \approx 1$, often monitoring the growth of numerous neighboring crystals. Quantitative extraction of $\alpha(T, \sigma_{surf})$ is therefore essentially impossible for these experiments. Similarly, growth measurements reported in [16] were made using quite large crystals at $p \approx 1$, so here also the growth was strongly diffusion-limited, making quantitative analysis to extract $\alpha(T, \sigma_{surf})$ quite difficult. Recent observations in [9] are likewise ill-suited for determining $\alpha(T, \sigma_{surf})$, owing to large diffusion effects.

In [17], the authors observed crystal growth velocities at $p \approx 0.3$ that were lower than expected from similar measurements at $p \approx 0$, concluding that α was strongly affected by the presence of air in their experiment. A possible alternative interpretation of their observations is simply that the supersaturation in the vicinity of the test crystal was somewhat smaller than calculated in their diffusion analysis, perhaps from the influence of unseen neighbor crystals. The key point here is that even a small error in the assumed supersaturation field would necessitate a large change in α to reproduce the observed growth velocities. We believe, therefore, that the claim made in [17] that α depends on air pressure is questionable, given the data and analysis presented.

Similar conclusions about the dependence of α on air pressure were reached by [18,19], but again we believe diffusion effects provide a viable alternative interpretation of their data. In our own experiments at $p \approx 1$, done with the apparatus described below, we have found that the diffusion corrections are exceedingly tricky to calculate, even with small test crystals and a greater attention to experimental systematics. One reliable conclusion we have reached from our $p \approx 1$ data is that the diffusion corrections are considerably more difficult to calculate than was previously appreciated.

The situation is somewhat better in [20], where the authors observed very low growth rates, as low as 0.3 nm/s. Since this is about 10 times lower than a typical v_{diff} in their experiments, the observed growth was partially kinetics limited. Some facets grew considerably faster than this minimum growth rate, however, so a detailed diffusion analysis would be needed to accurately determine σ_{surf} on the slower-growing facets.

2.2. Substrate interactions

When the attachment kinetics on a faceted ice surface include a substantial nucleation barrier, we have observed that this barrier may be lowered when the facet intersects a supporting substrate, a phenomenon that can be explained with the contact-angle model illustrated in Fig. 1. This can result in substantial systematic errors in growth measurements, since the ice-substrate contact angle is typically not well known and will depend on the cleanliness of the substrate. If a substrate surface is sufficiently hydrophilic, we have observed that the nucleation barrier can even be eliminated completely, giving unfaceted growth along the substrate.

Substrate interactions were previously observed in [19], where the authors noted that prism facets intersecting their substrate grew up to five times faster than prism facets not intersecting the substrate. It appears that measurements using intersecting facets were included in their final velocity data, however, suggesting that their results may have been seriously compromised by substrate interactions. The key point here is that substrate interactions can strongly affect growth measurements, to a degree that depends on the preparation and cleanliness of the substrate surface. Neglecting substrate interactions therefore casts considerable doubt on the accuracy of an ice growth measurement.

Substrate interactions were also apparently observed in [20], as the authors noted that facets contacting their capillary substrate sometimes grew much more rapidly than noncontacting facets. Substrate interactions may have substantially affected the measurements in [21,17,22] also, as the authors observed the growth of ice crystals with random orientations relative to their substrates.

For the experiments below, we spent some effort searching for a suitably hydrophobic coating that would eliminate or greatly reduce the effects of substrate interactions. Our search was unsuccessful, however, as all surface treatments we tried on our sapphire substrate tended to increase the substrate interaction problem. In the end we found that a carefully cleaned substrate showed the weakest substrate interactions, which were nevertheless often non-negligible.

2.3. Latent heat effects

Crystal heating effects arising from vapor deposition can be substantial for free-floating crystals, and their magnitude can be estimated by solving the double-diffusion problem (i.e. heat and particle diffusion) for the spherical case [7]. The overall effect is mainly to change the effective σ_{surf}, since the thermal conductivity of ice is high enough that the crystal itself has a uniform temperature, at least for small, slowly growing crystals. The double diffusion problem is nontrivial in general, so we believe that measurements made using freely floating crystals (e.g. [23–25,16]) are not well suited for estimating $\alpha(T, \sigma_{surf})$.

Fortunately, small crystals resting on a substrate are not greatly affected by latent heating, as the resulting crystal temperature rise is often negligible [7]. The growth of larger crystals may be affected by heating, however, leading to a rounding of faceted corners during growth [21].

3. Experimental procedures and growth data

For this investigation we sought to produce more accurate measurements of $\alpha(T, \sigma_{surf})$, improving upon previous work by

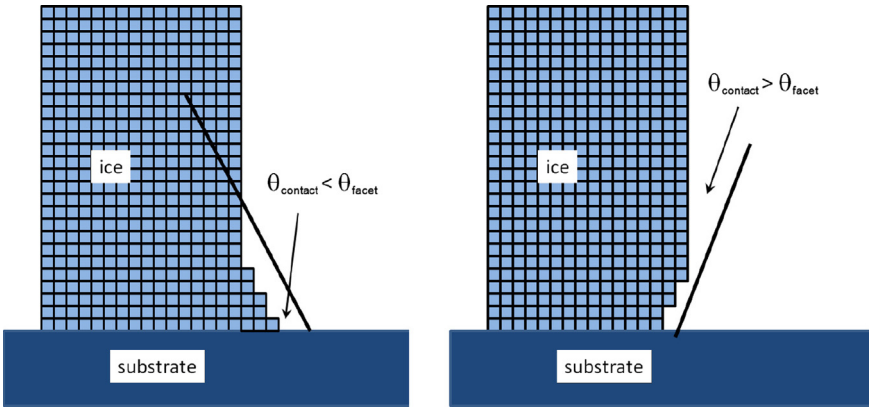

Fig. 1. If the ice/substrate contact angle $\theta_{contact}$ is less than the intersection angle θ_{facet} between the facet and the substrate, then the ice/substrate contact will act as a source of molecular steps on the intersecting ice facet, as seen in the diagram on the left. The presence of these molecular steps reduces the normal nucleation barrier on this facet, increasing the surface growth rate. If $\theta_{contact} > \theta_{facet}$, as in the diagram on the right, then the contact will not be a source of steps, and the nucleation barrier will remain unaffected. Since $\theta_{contact}$ depends on the chemical nature of the substrate, as well as on any chemical residue on an imperfectly cleaned substrate, substrate interactions can be somewhat unpredictable in ice growth experiments.

carefully reducing or eliminating the systematic errors described above. An idealized schematic diagram of our experimental set-up is shown in Fig. 2a. The top surface of the experimental chamber consisted of a sapphire "ice reservoir" at a uniform temperature T_{IR}, and a layer of ice crystals on its lower surface served as a source of water vapor. At the beginning of each measurement, an isolated test crystal was positioned below the center of the ice reservoir, resting on the bottom sapphire substrate surface held at temperature T_{subst}. The ice reservoir and the substrate were thermally isolated with a vertical spacing of 1.0 mm. The temperature difference $\Delta T = T_{IR} - T_{subst}$ determined the water vapor supersaturation seen by the test crystal. As ΔT was increased, the test crystal growth was monitored.

During a typical experimental run, we continuously nucleated small ice crystals in a much larger outer chamber containing ordinary laboratory air, where they grew while slowly falling to the bottom of the chamber. Typically $> 10^7$ of these micron-scale crystals were growing within the outer chamber at any given time, and the fall times were approximately 3–5 min. This cloud of freshly made, slowly growing crystals served as the source of seed crystals for our growth measurements. Thin plate-like crystals were grown with an outer chamber temperature near −13 °C, while columnar crystals were grown with a chamber temperature near −6 °C.

To select a test crystal, an inlet valve on the top of a smaller inner chamber was opened, and air carrying suspended ice crystals was drawn from the outer chamber through the inner chamber. Typically the inner chamber temperature was equal to T_{subst}. The operator rotated the substrate disk while observing the test region under the ice reservoir (see Fig. 2b), thus examining crystals that randomly landed on the substrate. After a suitable test crystal was identified and positioned, the inlet valve was closed and the pressure in the inner chamber was reduced so typically $p < 0.025$ during growth observations.

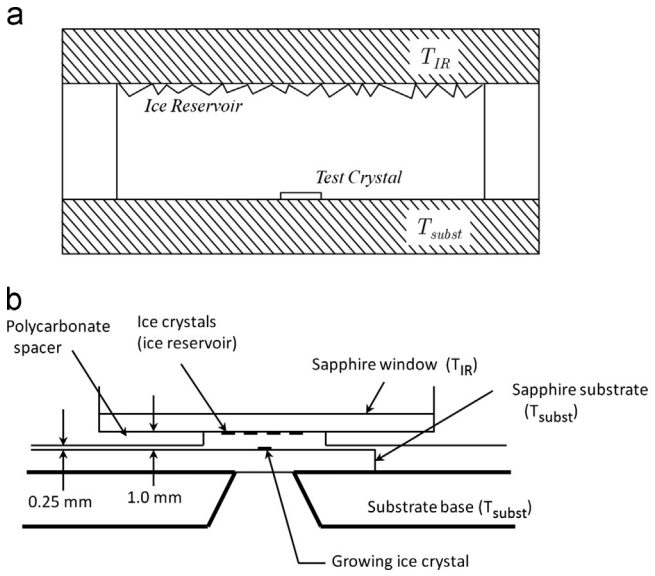

Fig. 2. (a) An idealized schematic of the inner sub-chamber of our experimental set-up. The top surface, covered with ice crystals, acts as a water vapor reservoir at temperature T_{IR} for a growing test crystal resting on the substrate at temperature T_{subst}. When $T_{IR} > T_{subst}$, growth rates are determined by measuring the thickness of the crystal (i.e. the distance between the substrate and the parallel top facet) as a function of time using optical interferometry, and by measuring the other crystal dimensions using optical microscopy viewing from below the substrate. The schematic in (b) shows the actual test chamber, located inside a larger vacuum chamber. The substrate disk can be rotated to bring test crystals into position under the ice reservoir. Additional experimental details are provided in [26].

Once the pressure was reduced, the operator first adjusted T_{IR} and observed the test crystal growing or evaporating slightly in order to determine the $\sigma = 0$ point. After this, ΔT was slowly increased to grow the test crystal. The thickness of the crystal – defined as the distance between the substrate and the parallel top facet – was determined using optical interferometry, while optical imaging was used to record the crystal size and morphology in the substrate plane. These data, along with the temperature difference ΔT, were all recorded as the crystal grew. At the end of a growth run, the crystal was evaporated away and another test crystal was selected. Sample crystals are shown in Figs. 3 and 4, and a more complete description of our apparatus can be found in [26].

The overall design of this experiment was not especially novel, being essentially similar to that described in [22], and it is a redesigned version of our previous experiment [27]. Many very significant improvements were made in the details, however, to ensure more accurate and reproducible measurements with much reduced systematic errors, including: (1) Only crystal facets parallel to, and thus not in contact with, the substrate were used to determine $\alpha(T, \sigma_{surf})$, thus eliminating systematic errors arising from substrate interactions, as described above; (2) crystal sizes typically $< 50\,\mu$m were used, with $p < 0.025$, and residual diffusion effects were corrected using Eq. (2), thus minimizing the systematic errors associated with diffusion-limited growth described above; (3) the ice reservoir was quite close to the test crystal, minimizing perturbations in the supersaturation field arising from unseen neighboring crystals; (4) residual chemical contamination was minimized by using low outgassing materials

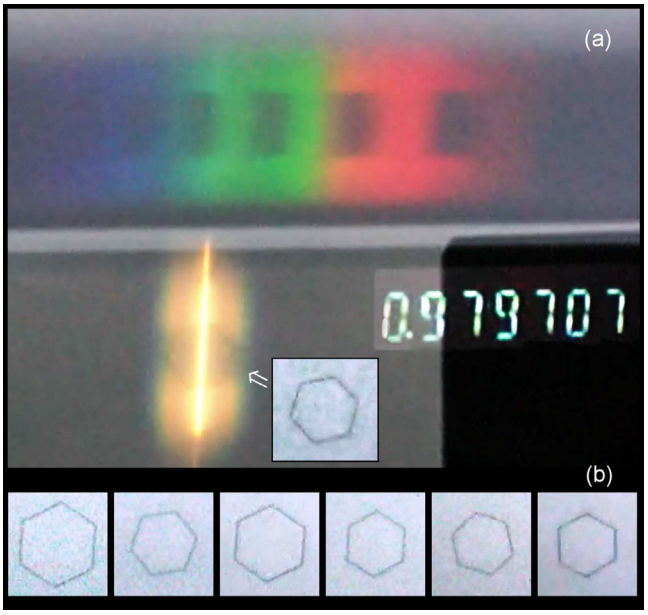

Fig. 3. The large top image (a) shows a sample video capture from our ice growth experiments. The lower left of this image gives a direct view of the test crystal, with a bright slit of broadband light incident upon it. The inset image shows a contrast-enhanced view of this simple plate-like crystal without the light from the slit; the distance between prism facets for this crystal was 36 μm. Heating from the incident slit light was negligible. The slit light reflected from the ice/substrate interface and the ice/air interface, and the combined light from both reflections was dispersed to produce the spectrum shown at the top of the image. The absolute thickness of the crystal was derived from the interference fringes in this spectrum, in this example giving a plate thickness of 3.0 μm. The digital display in the lower right gave a voltage from which T_{IR} could be derived. These three images (crystal, spectrum, and voltage) were optically combined onto the camera sensor to yield the overall image shown in (a), and a video was recorded for crystal growth analysis. The lower series of images (b) shows several sample crystals from one of many runs, all at the same scale as in (a), indicating the relatively small crystal-to-crystal size and morphological variations. Additional details of the experimental apparatus can be found in [26].

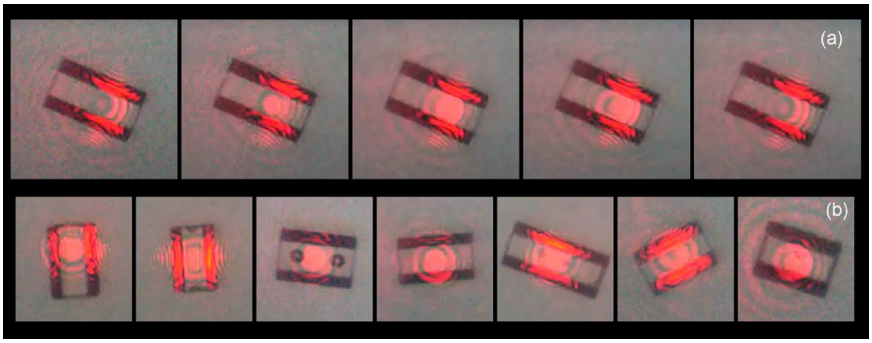

Fig. 4. Laser interferometry was used when measuring growth rates of the prism surface, as the distance between prism facets was too large to use the broadband interferometry technique shown in Fig. 3. The series of images in (a) shows a single ice prism, having an overall length of 63 μm, as it grew. Laser light reflected from the ice/substrate and ice/air interfaces, and the interference of these two reflections caused the intensity of the central laser spot to vary as the height of the upper prism facet above the substrate increased. Growth of the upper prism surface was determined by counting the laser intensity oscillations, while direct imaging yielded growth in the plane of the substrate. The lower series of images (b) shows several sample crystals, all at the same scale as in (a), indicating the relatively small crystal-to-crystal size and morphological variations. Additional details of the experimental apparatus can be found in [26].

in the vacuum chamber construction, placing temperature control elements and wiring outside the vacuum envelope, baking the chamber between runs, and cycling the chamber air between crystals; (5) precision temperature control [28] allowed us to determine the $\sigma=0$ point for each crystal to an accuracy of better than $\Delta\sigma\approx\pm 0.03\%$. The calculation relating σ to ΔT was validated by nucleating water droplets on the substrate (in the absence of any test crystals) and measuring ΔT at which the droplets were neither evaporating nor growing; (6) only crystals with near-perfect simple-prism morphologies were selected for measurement, as these were found to yield the most reproducible growth measurements; (7) crystals were grown only once and then discarded, as again we found that this practice yielded the most reproducible measurements; and (8) over 200 crystals were measured, on average eight for each facet at each temperature, to ensure data consistency and to test for systematic effects.

Fig. 5 shows sample data from our growth measurements of basal facets. As can be seen in these examples, the scatter in our velocity measurements was quite low, yielding accurate measurements of $v(\sigma_{surf})$ for individual crystals. All our growth measurements were well described using the functional form $\alpha(\sigma_{surf})=A\exp(-\sigma_0/\sigma_{surf})$, consistent with a polynucleation model. Attempts to use other growth models, for example the spiral dislocation model with $v\sim\sigma_{surf}^2$ shown in Fig. 5, yielded much poorer fits to the data.

All our basal growth data were furthermore well described by using $A=1$ in our parameterization of the polynucleation model, as is shown graphically in Fig. 6. For these data, therefore, we set $A=1$ and fit the $\alpha(\sigma_{surf})$ data for each crystal with the single adjustable parameter σ_0.

The main limitation in determining $\alpha(T,\sigma_{surf})$ came from crystal-to-crystal variations in growth, as seen in the histograms in Fig. 5. The source of these variations is not known, but could have been from minor crystal defects, greater than expected uncertainties in the inferred supersaturations, minor residual impurity chemical effects, or perhaps other causes.

In addition to the relatively minor variations in growth rates between crystals that we normally observed, we also found that a small number of crystals, less than 10%, exhibited growth behaviors that were far outside the norm. These "outlier" crystals, being clearly contaminated in some unknown way, perhaps by surface dislocations, were removed from further analysis.

Examining basal growth at −12 °C, where we measured the largest number of crystals, we found no correlation between growth rates and the areas of the basal facets, where the latter ranged from 10^{-9} to 8×10^{-9} m^2. The scatter in the data was fairly high, but this observation supports the hypothesis of a polynucleation model over a mononucleation model [8].

Fig. 7 shows additional sample data for growth of the prism facet. At temperatures $T\le-10$ °C the overall behavior was similar to that seen with the basal growth measurements, and the polynucleation model with $A=1$ provided a good fit of the data. For $T>-10$ °C, however, the measurements were no longer consistent with $A=1$, as is shown in Fig. 7b. For these data we fit for both A and σ_0 at each temperature.

We combined the individual $\sigma_{0,i}$ measurements for different crystals at a given temperature by weighting each measurement with an uncertainty $\delta\sigma_{0,i}$ estimated from the scatter in the raw data, producing a weighted mean $\langle\sigma_0\rangle$ along with an uncertainty estimate $\delta\langle\sigma_0\rangle$ for the mean [29]

$$\langle\sigma_0\rangle=\frac{\sum\sigma_{0,i}\delta\sigma_{0,i}^{-2}}{\sum\delta\sigma_{0,i}^{-2}}$$

$$(\delta\langle\sigma_0\rangle)^2=\frac{\sum(\sigma_{0,i}-\langle\sigma_0\rangle)^2\delta\sigma_{0,i}^{-2}}{(N_{eff}-1)\sum\delta\sigma_{0,i}^{-2}}$$

where $N_{eff}=(\sum\delta\sigma_{0,i}^{-2})/\delta\sigma_{0,\min}^{-2}$ is the effective number of points in the sample at each temperature. This method uses the scatter in the measurements along with the $\delta\sigma_{0,i}$ estimates to determine the error in the mean, and we believe it gave sensible uncertainty estimates. As a test we also formed unweighted averages (ignoring the $\delta\sigma_{0,i}$ estimates) and found that the results were not significantly different from the weighted averages. And in another test we fit $\langle\sigma_0\rangle$ to a data set that combined all the raw $\alpha(\sigma_{surf})$ data at a single temperature, and again the results were essentially equivalent to the weighted averages.

The final results from all our growth measurements are shown in Fig. 8. When we assumed $A=1$ in our fits, as described above, we assigned an approximate uncertainty of ±0.3 to A in Fig. 8, based on an overall assessment of the measurements. As we demonstrated above, the polynucleation model yielded an excellent fit to all our growth measurements, and the extracted coefficients $A(T)$ and $\sigma_0(T)$ then define the attachment coefficients $\alpha(T,\sigma_{surf})$ for the two principal facets.

4. Discussion and interpretation

Interpreting the results shown in Fig. 8 presents a significant challenge, as neither the structure nor the molecular dynamics of the ice surface are well understood, especially over this

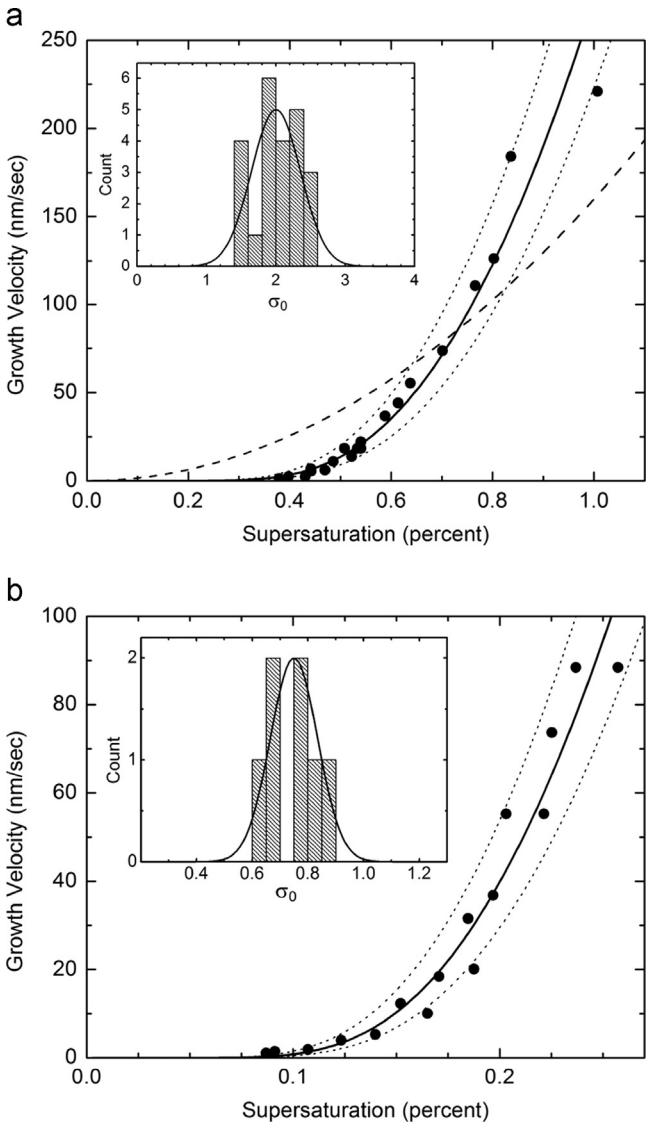

Fig. 5. (a) The growth velocity of the basal surface of a single ice crystal as a function of σ_{surf} at −12 °C, where data points were taken as the supersaturation was slowly increased. The line through the points gives the model $v = \alpha v_{kin}\sigma_{surf}$ with $\alpha = \exp(-\sigma_0/\sigma_{surf})$ and $\sigma_0 = 2.3\%$. The surrounding dotted lines show the same model with $\sigma_0 = 2.3 \pm 0.2\%$. The dashed line shows a spiral dislocation model with $v \sim \sigma_{surf}^2$, which gives a poor fit to the data. The inset graph shows an unweighted histogram of measured σ_0 values for 23 crystals. A weighted fit to these data gives an estimated mean $\langle\sigma_0\rangle = 1.95 \pm 0.15\%$. The set of plots in (b) show data taken at −5.15 °C. The model lines show $\sigma_0 = 0.64 \pm 0.06\%$ for a single crystal, while a weighted fit to all the data gives $\langle\sigma_0\rangle = 0.70 \pm 0.10\%$. Note that the errors in the mean are mainly determined by crystal-to-crystal variability, while raw velocity measurements of individual crystals often have quite low scatter.

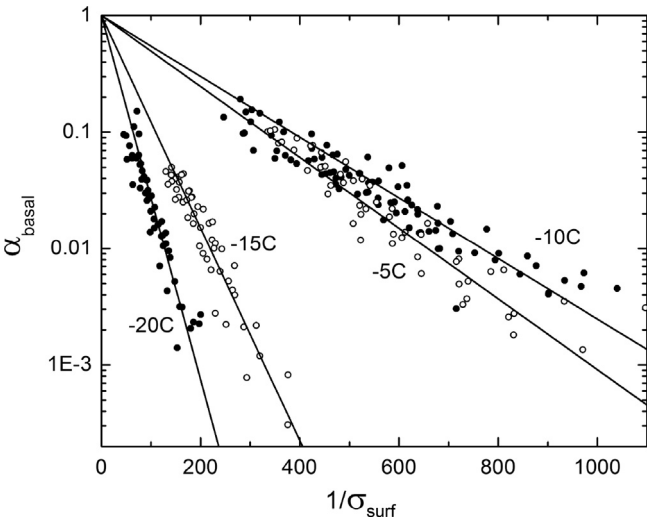

Fig. 6. Agreement with a polynucleation model can be seen more clearly by plotting measurements of $\alpha_{basal}(\sigma_{surf})$ versus σ_{surf}^{-1} as shown above. Then the model $\alpha = A\exp(-\sigma_0/\sigma_{surf})$ becomes a straight line with an intercept $A = \alpha(\sigma_{surf}^{-1} = 0)$, and again we see excellent agreement with this functional form. The convergence to a common intercept demonstrates that these growth measurements were well described by this model using $A = 1$. A similar convergence to a common intercept has been observed with the growth of helium crystals [31].

temperature range near the melting point. We offer the following conclusions and observations:

(1) The measured attachment coefficients for both principal facets are well described by a polynucleation model with the simplified parameterization $\alpha(T, \sigma_{surf}) = A\exp(-\sigma_0/\sigma_{surf})$. This supports the existing evidence [9] that layer nucleation is the dominant source of molecular steps in faceted ice crystal growth, and that dislocations play at most a minor role in the basic growth behavior of ice facet surfaces.

(2) Embracing the polynucleation model, we reduced our data from a set of velocity measurements $v(T, \sigma_{surf})$ to a substantially simpler set of coefficients $A(T)$ and $\sigma_0(T)$ for the principal facets. Presenting the data in this way brings us a substantial step closer to addressing the underlying physical processes governing ice growth behavior.

(3) The measured $\sigma_0(T)$ for each facet immediately yields the terrace step energy $\beta(T)$ from an application of classical 2D nucleation theory in the polynucleation model [8]. A plot of $\beta(T)$ thus extracted from our data is shown in Fig. 9. We note from the scale on the right side of Fig. 9 that $\beta(T)$ is much smaller than $\beta_0 = \gamma a \approx 3.5 \times 10^{-11}$ J/m, the product of the surface energy $\gamma \approx 0.11$ J/m^2 of the ice/vapor interface and the nominal molecular step height $a \approx 0.32$ nm, which is an upper limit on the step energy.

(4) We note that the step energy $\beta(T)$ is a fundamental property of a crystalline facet surface, in much the same way that the surface energy is a fundamental quantity. It is also an equilibrium quantity, even though it was derived here from the dynamical process of crystal growth. As an equilibrium, molecular-scale quantity, the step energy $\beta(T)$ may be amenable to calculation using perturbation techniques or molecular dynamics simulations. The observed strong temperature dependence in $\beta(T)$, as well as the difference between facets, may thus yield important insights into the equilibrium ice surface structure as a function of temperature.

(5) It is likely that the two measured $\beta(T)$ ultimately derive from temperature-dependent structural changes associated with surface melting on the principal facets. Surface melting is known to produce a quasiliquid layer on the ice surface over this temperature range, with a thickness that is strongly temperature dependent [30]. Surface melting is itself only poorly understood, but our measurements of $\beta(T)$ suggest that attempts to calculate step energies should be included in more general investigations of ice surface structure in the presence of surface melting.

(6) All our basal growth measurements, as well as our prism growth measurements with $T \le -10$ °C, are well described with $A = 1$ in the polynucleation model. We do not fully understand the preference for $A = 1$, although the limit $\alpha \to 1$ when $\sigma_{surf} \gg \sigma_0$ may simply reflect an effective kinetic roughening phenomenon that yields unimpeded growth in this limit [8]. A similar convergence at high growth rates has been seen in measurements of helium crystals [31].

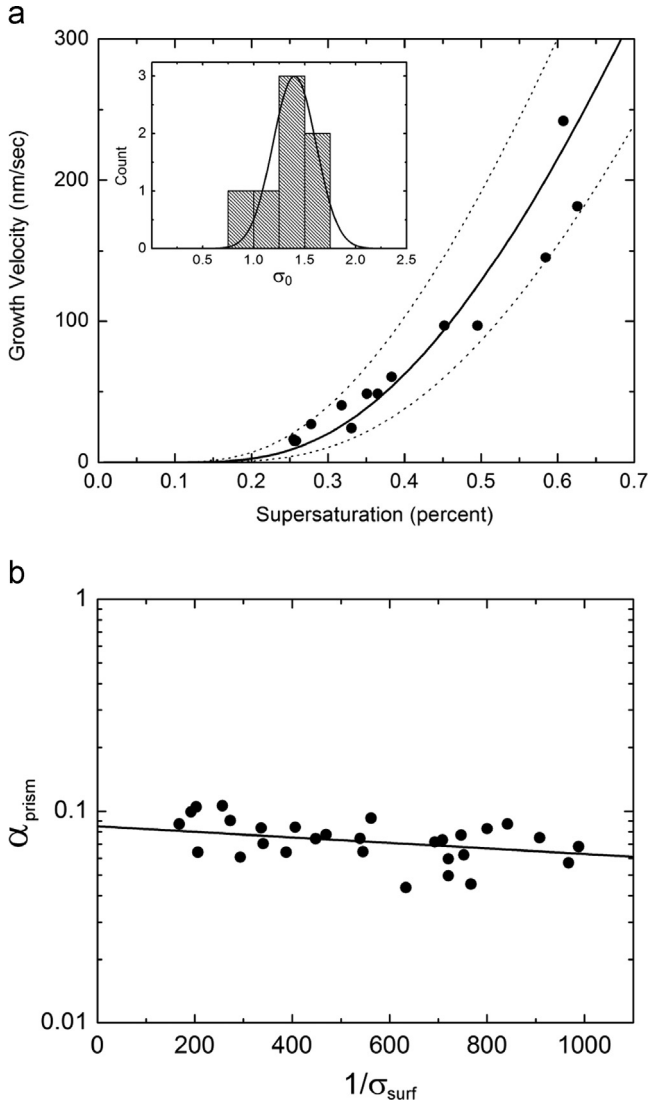

Fig. 7. (a) Another set of plots similar to those shown in Fig. 5, this time showing growth measurements of the prism facet at −8.3 °C. The model lines show $\sigma_0 = 1.0 \pm 0.2\%$, while a weighted fit to all the data gives $\langle\sigma_0\rangle = 1.4 \pm 0.3\%$. The plot in (b) shows displays combined measurements of four crystals growing at −3 °C, showing α_{prism} as a function of σ_{surf}^{-1} for the prism facet. The model line shows $\alpha = A\exp(-\sigma_0/\sigma_{surf})$ with $A = 0.085$ and $\sigma_0 = 0.03\%$. Extrapolating the data in this plot to $\sigma_{surf}^{-1} = 0$ demonstrates that the −3 °C prism growth data are not consistent with an $A = 1$ model.

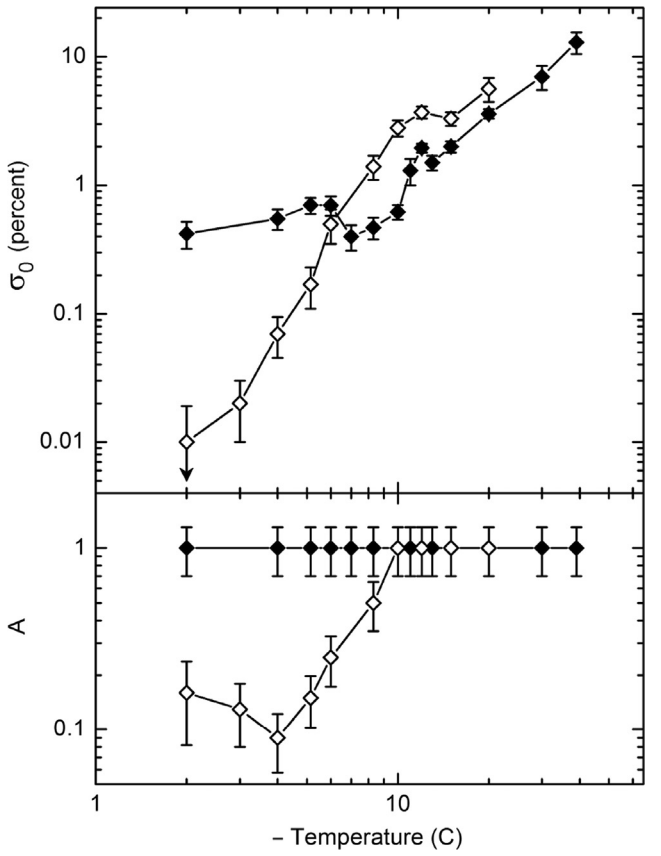

Fig. 8. Combined final measurements of the growth behavior of the basal (solid points) and prism (open points) facet surfaces of ice crystals. The attachment coefficients were parameterized using $\alpha(T,\sigma_{surf}) = A\exp(-\sigma_0/\sigma_{surf})$, and the plots show the parameters $A(T)$ and $\sigma_0(T)$ extracted from our data for both principal facets.

(7) Our prism data for $T > -10$ °C require $A < 1$, and we do not understand the origin of this observation. Calculating the prefactor in the polynucleation model is nontrivial, depending on the lateral growth velocity of molecular steps on the facet surface and other factors [8]. Furthermore, these calculations assume a surface structural model that may be too simplistic for the ice case, when significant surface melting is present.

(8) Above $T \approx -5$ °C we find that $\sigma_{0,basal} \gg \sigma_{0,prism}$, in a temperature regime where we would expect to find a thick quasiliquid layer on the ice surface. This is consistent with the growth behavior of ice from liquid water, where faceted basal surfaces grows much more slowly than prism surfaces at low supercoolings. It also suggests that the nucleation barrier seen in basal growth from vapor at these high temperatures arises at the interface between crystalline ice and the quasiliquid layer at the surface. Quantitatively relating the crystal growth rates from water vapor and from liquid water may be a tractable theoretical problem, since the surface attachment kinetics at the liquid/solid and the quasiliquid/solid interfaces should be similar in the limit of a thick quasiliquid layer.

(9) At −15 °C we see from Fig. 8 that $\alpha_{basal} > \alpha_{prism}$ at all supersaturations, which is at odds with the formation of very thin plate-like crystals at this temperature, as seen in the morphological studies. The explanation for this may lie in the fact that our measurements give $\alpha(T,\sigma_{surf})$ only for flat facet surfaces. If σ_0 on the edge of a thin plate is substantially lower than σ_0 on a broad prism facet, a hypothesis put forth in [32] as *structure-dependent attachment kinetics* (SDAK), then this could explain the formation of thin plates at −15 °C in a way that is consistent with the flat-facet $\alpha(T,\sigma_{surf})$ measurements. With our improved picture of $\alpha(T,\sigma_{surf})$ for flat facet surfaces, targeted growth experiments can further explore and quantify the SDAK hypothesis.

(10) Our measurements of $\sigma_0(T)$ for the principal facets are in rough agreement with the $\sigma_{crit}(T)$ measurements presented in [20]. As discussed above, the data in [20] are partially influenced by diffusion effects, so a direct quantitative comparison between $\sigma_0(T)$ and $\sigma_{crit}(T)$ may not be strictly accurate. Nevertheless, if one assumes that the discrepancy for the prism growth at −15 °C is an SDAK effect in [20], then the remaining overall trends in the two data sets are roughly similar.

In summary, we have measured growth rates of the principal facets of ice as a function of supersaturation in the temperature range $-40 < T < -2$ °C. By reducing systematic errors that

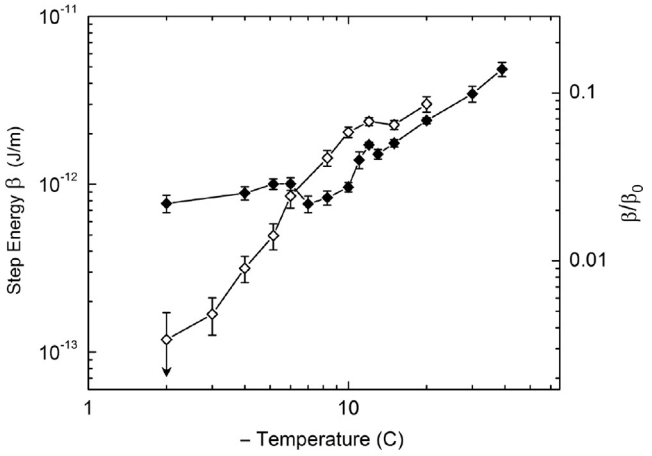

Fig. 9. The molecular step energy $\beta(T)$ on a ice surface, extracted from our measurements of $\sigma_0(T)$ using classical nucleation theory, for the basal (solid points) and prism (open points) facets. The scale on the right compares β with $\beta_0 = \gamma a$, where γ is the surface energy and a is the step height, as β_0 gives a nominal step energy for a sharp (unrelaxed) molecular step.

adversely affected earlier experiments, our measurements have yielded a much clearer picture of the ice attachment coefficients $\alpha(T, \sigma_{surf})$. These data help open a path for more detailed investigations of the ice surface structure, quantitative calculation of molecular step energies on the facet surfaces, and eventually an improved understanding of the general physical processes governing crystal growth dynamics.

Acknowledgements

This work was supported in part by the California Institute of Technology and the Caltech-Cambridge Exchange (CamSURF) program.

References

[1] D. Pan, L.M. Liu, B. Slater, et al., Melting the ice: on the relation between melting temperature and size for nanoscale ice crystals, ACS Nano 5 (2011) 4562–4569.
[2] M.M. Conde, C. Vega, A. Patrykiejew, The thickness of a liquid layer on the free surface of ice as obtained from computer simulation, Journal of Chemical Physics 129 (014702) (2008).
[3] Y. Furukawa, H. Nada, Anisotropic surface melting of an ice crystal and its relationship to growth forms, Journal of Physical Chemistry B 101 (1997) 6167–6170.
[4] M.A. Carignano, P.B. Shepson, I. Szleifer, Molecular dynamics simulations of ice growth from supercooled water, Molecular Physics 103 (2005) 2957–2967.
[5] H. Kang, Chemistry of ice surfaces: elementary reaction steps on ice studied by reactive ion scattering, Accounts of Chemical Research 38 (2005) 893–900.
[6] P. Parent, et al., Hcl adsorption on ice at low temperature: a combined x-ray absorption, photoemission and infrared study, Physical Chemistry Chemical Physics 13 (2011) 7111–7177.
[7] K.G. Libbrecht, The physics of snow crystals, Reports on Progress in Physics 68 (2005) 855–895.
[8] Y. Saito, Statistical Physics of Crystal Growth, World Scientific Books, 1996.
[9] C.A. Knight, Ice growth from the vapor at −5 °C, Journal of the Atmospheric Sciences 69 (2012) 2031–2040.
[10] G. Sazaki, et al., Elementary steps at the surface of ice crystals visualized by advanced optical microscopy, Proceedings of the National Academy of Sciences 107 (2010) 19702–19707.
[11] U. Nakaya, Snow Crystals, Harvard University Press, Cambridge, 1954.
[12] M. Bailey, J. Hallett, A comprehensive habit diagram for atmospheric ice crystals: confirmation from the laboratory, airs ii, and other field studies, Journal of the Atmospheric Sciences 66 (2012) 2888–2899.
[13] T. Kuroda, R. Lacmann, Growth kinetics of ice from the vapour phase and its growth forms, Journal of Crystal Growth 56 (1982) 189–205.
[14] J. Nelson, Growth mechanisms to explain the primary and secondary habits of snow crystals, Philosophical Magazine 81 (2001) 2337–2373.
[15] T. Kuroda, Rate determining processes of growth of ice crystals from the vapour phase—part i: theoretical considerations, Journal of the Meteorological Society of Japan 62 (1984) 1–11.
[16] T. Takahashi, et al., Vapor diffusional growth of free-falling snow crystals between −3 and −23 °C, Journal of the Meteorological Society of Japan 69 (1991) 15–30.
[17] T. Kuroda, T. Gonda, Rate determining processes of growth of ice crystals from the vapour phase—part ii: investigation of surface kinetic processes, Journal of the Meteorological Society of Japan 62 (1984) 563–572.
[18] W. Beckmann, Interface kinetics of the growth and evaporation of ice single crystal from the vapor phase – part iii: measurements under partial pressures of nitrogen, Journal of Crystal Growth 58 (1982) 443–451.
[19] W. Beckmann, R. Lacmann, A. Blerfreund, Growth rates and habits of ice crystals grown from the vapor phase, Journal of Physical Chemistry 87 (1983) 4142–4146.
[20] J. Nelson, C. Knight, Snow crystal habit changes explained by layer nucleation, Journal of the Atmospheric Sciences 55 (1998) 1452–1465.
[21] D. Lamb, W.D. Scott, Linear growth rates of ice crystals grown from the vapor phase, Journal of Crystal Growth 12 (1972) 21–31.
[22] T. Sei, T. Gonda, The growth mechanism and the habit change of ice crystals growing from the vapor phase, Journal of Crystal Growth 94 (1989) 697–707.
[23] A. Yamashita, K.K. Noto, Studies on the ice crystals using a large diffusion chamber, Meteorological Society of Japan 123 (1974) 47–97.
[24] T. Kobayashi, T. Kuroda, Snow Crystals: Morphology of Crystals—Part B, Terra Scientific, Tokyo, 1987.
[25] K.G. Libbrecht, H. Yu, Crystal growth in the presence of surface melting: supersaturation dependence of the growth of columnar ice crystals, Journal of Crystal Growth 222 (2001) 822–831.
[26] K.G. Libbrecht, An improved apparatus for measuring the growth of ice crystals from water vapor between −40°C and 0°C, arXiv: 2011; (1109.1511).
[27] K.G. Libbrecht, Growth rates of the principal facets of ice between −10 °C and −40 °C, Journal of Crystal Growth 247 (2003) 530–535.
[28] K.G. Libbrecht, A versatile thermoelectric temperature controller with 10 mk reproducibility and 100 mk absolute accuracy, Review of Scientific Instruments 80 (126107) (2009).
[29] J.R. Taylor, An Introduction to Error Analysis, 2nd edition, University Science Books, 1997.
[30] J.G. Dash, A.W. Rempel, J.S. Wettlaufer, The physics of premelted ice and its geophysical consequences, Review of Modern Physics 78 (2006) 695–741.
[31] P.E. Wolf, F. Gallet, S. Balibar, E. Rolley, P. Nozieres, Crystal growth and crystal curvature near roughening transitions in hcp 4He, Journal de Physique 46 (1985) 1987–2007.
[32] K.G. Libbrecht, Explaining the formation of thin ice-crystal plates with structure-dependent attachment kinetics, Journal of Crystal Growth 258 (2003) 168–175.